HHS Public Access

Author manuscript

Acta Biomater. Author manuscript; available in PMC 2018 January 15.

Published in final edited form as:

Acta Biomater. 2017 January 15; 48: 120–130. doi:10.1016/j.actbio.2016.10.037.

A robust vitronectin-derived peptide for the scalable long-term expansion and neuronal differentiation of human pluripotent stem cell (hPSC)-derived neural progenitor cells (hNPCs)

Divya Varun[1], **Gayathri Rajaram Srinivasan**[1], **Yi-Huan Tsai**[1], **Hyun-Je Kim**[1], **Joshua Cutts**[1], **Francis Petty**[1], **Ryan Merkley**[2], **Nicholas Stephanopoulos**[2], **Dasa Dolezalova**[3], **Martin Marsala**[4], and **David A. Brafman**[1,*]

[1]School of Biological and Health Systems Engineering, Arizona State University

[2]School of Molecular Sciences and Biodesign Institute Center for Molecular Design and Biomimetics, Arizona State University

[3]Department of Histology and Embryology, Faculty of Medicine, Masaryk University, Brno, Czech Republic

[4]Department of Anesthesiology, University of California - San Diego

Abstract

Despite therapeutic advances, neurodegenerative diseases and disorders remain some of the leading causes of mortality and morbidity in the United States. Therefore, cell-based therapies to replace lost or damaged neurons and supporting cells of the central nervous system (CNS) are of great therapeutic interest. To that end, human pluripotent stem cells (hPSC) derived neural progenitor cells (hNPCs) and their neuronal derivatives could provide the cellular 'raw material' needed for regenerative medicine therapies for a variety of CNS disorders. In addition, hNPCs derived from patient-specific hPSCs could be used to elucidate the underlying mechanisms of neurodegenerative diseases and identify potential drug candidates. However, the scientific and clinical application of hNPCs requires the development of robust, defined, and scalable substrates for their long-term expansion and neuronal differentiation. In this study, we rationally designed a vitronectin-derived peptide (VDP) that served as an adhesive growth substrate for the long-term expansion of several hNPC lines. Moreover, VDP-coated surfaces allowed for the directed neuronal differentiation of hNPC at levels similar to cells differentiated on traditional extracellular matrix protein-based substrates. Overall, the ability of VDP to support the long-term expansion and directed neuronal differentiation of hNPCs will significantly advance the future translational application of these cells in treating injuries, disorders, and diseases of the CNS.

Graphical Abstract

*CORRESPONDING AUTHOR: David Brafman, (480) 727-2859, David.Brafman@asu.edu, 501 E. Tyler Mall, ECG 334A, Tempe, AZ 85287.

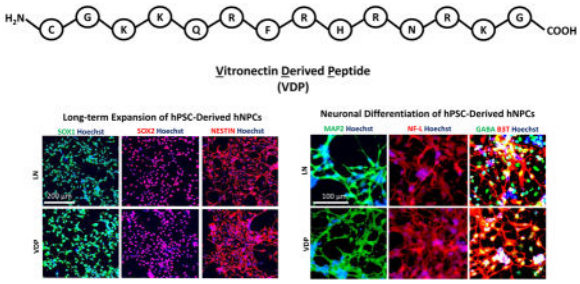

Keywords

Human pluripotent stem cells; human neural progenitor cells; peptide; defined conditions

1. INTRODUCTION

The lack of effective therapies for neurological injuries, disorders, and diseases of the central nervous system (CNS) creates an enormous burden on society. Current pharmacological-based treatments of these diseases are inadequate as they only treat symptoms and not the underlying disease etiology—the damage, degeneration, and death of the neurons and supporting cell types of the CNS. Stem-cell based technologies have emerged as a promising approach for the study and treatment of these diseases (1–3). Specifically, human pluripotent stem cell (hPSC)-derived neural progenitor cells (hNPCs), a multipotent cell population that is capable of extensive *in vitro* expansion and subsequent differentiation into the various cell types that comprise the CNS, could provide an unlimited source of cells for such cell-based therapies (2, 4–6). In fact, recent research supports the use of these cells as the basis for regenerative medicine therapies to reverse or arrest neurodegeneration or replace dead or diseased neural cells (2, 3, 6–8). In addition, generating neural cells from human disease specific hPSCs is of particular interest because animal models of neurodegenerative diseases do not display important pathological hallmarks and do not adequately model the complex genetics associated with human neurodegenerative diseases (9–12). Furthermore, such hPSC-based ‘disease-in-a-dish’ models can be used to discover new drug targets and develop efficacious therapeutic compounds (9). However, to realize the full potential of hNPCs in these applications the development of defined, robust, and scalable culture conditions for their expansion and neuronal differentiation are needed.

The extracellular matrix (ECM) is a dynamic component of the cell microenvironment that not only functions to support cell attachment and growth but also regulates cell differentiation and fate (13, 14). To that end, we and others have investigated the effects of various extracellular matrix proteins (ECMPs) on the self-renewal and differentiation of hPSCs (15–18). As it relates to the culture of hNPCs, the most common ECMP-based culture substrates, such as Matrigel™ and laminin (19, 20), are difficult to isolate, expensive, biochemically undefined, subject to batch-to-batch inconsistencies, and contain potentially hazardous xenogeneic components, thereby limiting the scientific and clinical application of cells cultured with these substrates. In addition, ECMPs are structurally complex molecules that contain several receptor binding motifs, making it difficult to elucidate and control their

biological function. By comparison, peptide-based materials consisting of short amino acid sequences derived from the cell binding domains of ECMPs are inexpensive, completely defined, and easily produced. As such, several peptide-based substrates have been developed for the long-term culture and directed differentiation of hPSCs (21–27). However, completely defined peptide-based substrates that support the adhesion, growth, and differentiation of hNPCs have not been previously developed.

In this study, we characterized the ECM and cell surface integrin profile of hNPCs to rationally design peptide-based substrates for the growth and differentiation of hNPCs. Of the peptides tested, we identified one 14 amino acid long peptide derived from the cell-binding domain of vitronectin (28) that provides for the expansion and neuronal differentiation of hNPCs. Moreover, this peptide, referred to as vitronectin-derived peptide (VDP), is easily coated onto tissue-culture treated polystyrene (TCPS) plates and supports the long-term propagation and directed neuronal differentiation of multiple hNPC lines in completely defined medium conditions. Overall, VDP is a completely defined and scalable substrate that support the long-term expansion and directed neuronal differentiation of hNPCs in quantities necessary for their scientific and clinical applications.

2. MATERIALS AND METHODS

2.1 Human pluripotent stem cell (hPSC) culture

All media components were from Life Technologies unless otherwise noted. For hPSC culture on mouse embryonic fibroblast (MEF) feeders, the following media were used: MEF (1X high glucose DMEM, 10% fetal bovine serum, 1% (v/v) L-glutamine penicillin/streptomycin). H9/HES3/RiPSC hPSCs (1X DMEM-F12, 20% (v/v) Knockout Serum Replacement, 1% (v/v) non-essential amino acids, 0.5% (v/v) glutamine, 120 μM 2-mercaptoethanol [Sigma]). HSF4 (1X high glucose DMEM+L-Glutamine, 20% (v/v) Knockout Serum Replacement, 1% (v/v) non-essential amino acids, 100 μM 2-mercaptoethanol). All hPSC lines were maintained on feeder layers of mitotically inactivated MEFs (Millipore). All hPSC cultures were supplemented with 30 ng/ml FGF2 (Life Technologies). For culture of hPSCs in the absence of feeders, hPSCs were grown on Matrigel (BD Biosciences) or Geltrex (Life Technologies) in the presence of MEF-conditioned media (MEF-CM; produced by culturing hPSC medium on MEFs for 24 hr followed by sterile filtering), mTeSR2 (Stem Cell Technologies), or Essential 8 (Life Technologies). Cells were routinely passaged every 4–5 days with Accutase and 5 μM Rho kinase inhibitor (Y-27632) (Stemgent) to aid in cell survival. HPSCs were differentiated to early endoderm (EN), mesoderm (ME), and ectoderm (EC) cell populations as previously described (29).

2.2 Human neural progenitor cell (hNPC) generation, expansion, and differentiation

H9-, HES3-, and RiPSC-hNPCs were derived as previously described (30). Briefly, to initiate neural differentiation hPSCs were cultured in feeder-free conditions for a minimum of 2 passages. Cells were then detached with Accutase and resuspended in neural induction media [1X DMEM-F12, 1% (v/v) N2 supplement (Life Technologies), 1% (v/v) B27 supplement (Life Technologies)] supplemented with 5 μM Rho kinase inhibitor (Y-27632),

50 ng/ml recombinant mouse Noggin (R&D Systems), 0.5 μM Dorsomorphin (Tocris Bioscience)]. Next, 1–2 × 10^6 cells were pipetted to each well of a 6-well ultra-low attachment plate (Corning). The plates were then placed on an orbital shaker set at 95 rpm in a 37°C/5% CO_2 tissue culture incubator. The next day, the cells formed spherical cultures (embryoid bodies [EBs]) and the media was changed to neural induction media with 50 ng/ml recombinant mouse Noggin and 0.5 μM Dorsomorphin. Half of the media was subsequently changed every day. After 5 days in suspension culture, the EBs were then transferred to a 10 cm dish (1–2 6 wells per 10 cm dish) coated with Matrigel. The plated EBs were cultured in neural induction media with 50 ng/ml recombinant mouse Noggin and 0.5 μM Dorsomorphin for an additional 5–7 days. Neural rosettes were cut out by dissection under an EVOS (Life Technologies) microscope. Rosettes were then plated on surfaces that had be coated first with poly-L-ornithine (PLO) and then with mouse laminin (LN; 5 μg/mL) as described as follows: Tissue culture plates were coated with 10 μg/mL PLO at 37°C for 4 hours. After 4 hours of incubation, the PLO solution was aspirated and the plates were washed 3 times with PBS. The plates were then coated with 5 μg/mL LN at at 37°C overnight and washed 3 times with PBS prior to use. In the manuscript and figures these plates are simply referred to as LN-coated. Plated neural rosettes were cultured in LN-coated dishes in neural induction media supplemented with 30 ng/ml mouse FGF2 and 30 ng/ml mouse EGF (R&D systems). HSF4-hNPCs were generated as previously described (31). For routine maintenance, hNPCs were passaged onto LN-coated plates at a density of 1–5 × 10^4 cells/cm ^{2} in neural induction media supplemented with 10 ng/ml mouse FGF2 and 10 ng/ml mouse EGF2. For neuronal differentiation, hNPCs were grown to confluence and the media was changed to neuronal differentiation media [1X DMEM-F12, 0.5% (v/v) N2 supplement (Life Technologies), 0.5% (v/v) B27 supplement (Life Technologies)] with 20 ng/ml BDNF (R&D Systems), 20 ng/ml GDNF (R&D Systems), 1 μM DAPT (Tocris Bioscience), and 0.1 mM dibutyrl-cAMP (db-cAMP).

2.3 HNPC culture and neuronal differentiation on peptide substrates

All peptides were custom synthesized by AnaSpec. The linear peptide sequences were synthesized on a resin using standard Fmoc chemistries. Analysis of the peptides by analytical HPLC and MALDI-TOF confirmed that the peptides had the correct expected masses. The peptides were then subjected to HPLC using C18 columns to remove any impurities. Analytical HPLC and ESI-MS were used to confirm the purity and mass, respectively. The solvents used to dissolve the peptide were Buffer A (0.1% TFA in water) and Buffer B (0.1% TFA in acetonitrile). Over a run time of 8.5 min, the step-wise gradient increased the percentage of Buffer B from 1% to 30%. The analytical HPLC was monitored at 220 nm. Peptide sequences are listed in Supplementary Table 1. Peptide surfaces were prepared by reconstituting lyophilized peptide in sterile water and coating multi-well plates overnight at 37°C. Peptide-coated plates were washed twice with PBS prior to culture. HNPC culture and neuronal differentiation was performed in a similar manner as described for PLO/LN-coated surfaces. For conjugation of Fluorescein-5-maleimide (F5M) to VDP coated surfaces, 1 mM of F5M was incubated with peptide coated surfaces at 37°C for 48 hours. Peptide coated surfaces were rinsed twice with 10 mM PBS + 130 mM NaCl to remove free peptide and dye. Fluorescence images of each well at 20 x were obtained using an EVOS FL Cell Imaging System using the GFP channel (ex/em: 470/510 nm) at 30%

brightness and 120 ms exposure time. To assess for the effect of integrin αv blocking on hNPC adhesion to VDP, hNPCs were incubated in suspension with 5 μg/ml integrin αv blocking antibody (Millipore MAB1953Z) for 15 min at 37OC prior to plating onto VDP- or LN-coated substrates. Cell counts and images were acquired after 48 hours of culture. To assess for the effect of disruption of cell surface proteoglycan-substrate interactions, hNPCs were incubated in suspension with (i) 2 U/ml chondroitinase ABC (Sigma) or (ii) 500 μg/ml heparin (Sigma) for 1 hr at 37OC prior to plating onto VDP- or LN-coated surfaces. Cell counts and images were acquired after 48 hours of culture.

2.4 Quantitative PCR (qPCR)

RNA was isolated from cells using the NucleoSpin RNA Kit (Clontech). Reverse transcription was performed with qScript cDNA Supermix (Quanta Biosciences) or iScript RT Supermix (Bio-Rad). Quantitative PCR was carried out using TaqMan Assays or SYBR green dye on a Bio-Rad CFX96 or CFX384 Touch™ Real-Time PCR Detection System. QPCR experiments run with TaqMan Assays were carried out using TaqMan Gene Expression Master Mix (Life Technologies). QPCR experiments run with SYBR green dye were carried out using iTaq Universal SYBR Green Supermix (Bio-Rad). For the qPCR experiments run with TaqMan® Assays a 10 min gradient to 95 °C followed by 40 cycles at 95 °C for 5 s and 60 °C for 30 s was used. For qPCR experiments run with SYBR green dye, a 2 min gradient to 95 °C followed by 40 cycles at 95 °C for 5 s and 60 °C for 30 s was used. The list of TaqMan® assays and primer sequences used is provided in Supplementary Table 2. Gene expression was normalized to 18S rRNA levels. Delta Ct values were calculated as C^{target} - Ct^{18s}. Relative fold changes in gene expression were calculated using the $2^{-\Delta\Delta Ct}$ method (32).

2.5 Immunofluorescence

Cultures were gently washed twice with stain buffer (BD Biosciences) prior to fixation. Cultures were then fixed for 15 min at room temperature (RT) with BD Cytofix Fixation Buffer (BD Biosciences). The cultures were then washed twice with staining buffer and permeabilized with BD Phosflow Perm Buffer II (BD Biosciences) for 30 min at 4°C. Cultures were then washed twice with stain buffer. Primary antibodies were incubated overnight at 4°C and then washed twice with stain buffer at RT. Secondary antibodies were incubated at RT for 1 hr. Antibodies used are listed in Supplementary Table 3. Nucleic acids were stained for DNA with Hoechst 33342 (2 μg/ml; Life Technologies) for 5 min at RT and then washed twice with stain buffer. Imaging was performed using an automated confocal microscope (Olympus Fluoview 1000 with motorized state) or EVOS microscope (Life Technologies)

2.6 Flow cytometry

Cells were dissociated with Accutase for 5 min at 37°C, triturated, and passed through a 40 μm cell strainer. Cells were then washed twice with stain buffer (BD Biosciences) and resuspended at a maximum concentration of 5×10^6 cells per 100 μl. For staining of extracellular membrane proteins, one test volume of antibody was added for each 100 μl cell suspension. Cells were stained for 30 min on ice, washed, and resuspended in stain buffer. For staining of intracellular proteins, cells were fixed for 10 min on ice with BD Cytofix

Fixation Buffer (BD Biosciences). The cells were then washed twice with stain buffer and permeabilized with BD Phosflow Perm Buffer II (BD Biosciences) for 30 min on ice. Cells were then washed twice with stain buffer and one test volume of antibody was added for each 100 μl of cell suspension. Cells were stained for 30 min on ice, washed, and resuspended in stain buffer. Cells were analyzed on a FACSCanto (BD Biosciences) or ACCURI C6 (BD Biosciences). Antibodies and isotype negative controls are listed in Supplementary Table 3.

2.7 Population doubling time

Population doubling time of hNPCs was calculated using the following equation: PDT (h) = (T2 − T1)/(3.32 * [log(N2) − log(N1)]).

2.8 Statistical analysis

Data were analyzed using Student's t-test and ANOVA statistical methods. Where appropriate, a Bonferroni post hoc correction was employed. A p-value < 0.05 was considered significant. Unless otherwise notes, all data are displayed as mean ± standard error of the mean (S.E.M.).

3. RESULTS

3.1 Identification of defined peptide-based substrates for the expansion of hNPCs

We have previously developed a serum free protocol that allows for the robust generation of hNPCs from several hPSC lines (30). Briefly, hNPCs were generated through the stepwise formation of embryoid bodies (EBs) and neuroepithelial-like rosettes. After manual dissection from EB-derived rosettes, hNPCs were replated and maintained as proliferative, multipotent cells. Upon continuous culture with FGF2 and EGF on laminin (LN)-coated surfaces, hNPCs proliferated extensively and maintained high levels of expression of SOX1 and NESTIN (Supplementary Figure 1A). Subsequent differentiation of hNPCs to neurons was achieved through the withdrawal of FGF2 and EGF and addition of BDNF, GDNF, dibutyrl-cAMP (db-cAMP), and the Notch inhibitor DAPT. After four weeks of treatment, cells acquired a neuronal morphology and expressed high levels of the pan-neuronal markers such as β-Tubulin-III (B3T; Supplementary Figures 1B).

The extracellular matrix (ECM) is complex network of extracellular matrix proteins (ECMPs) that provides a scaffold for cell adhesion and growth (13, 14, 33). Integrins are a family of cell surface receptors that mediate binding to these ECMPs (13, 33). To rationally design a set of defined peptides that could mimic the ECM and promote the adhesion as well as growth of hNPCs, we measured the expression levels of various integrins and components of the ECM in undifferentiated hESCs, hNPCs, as well as early endoderm (EN), mesoderm (ME), and ectoderm (EC) cell populations differentiated from hESCs (Figure 1A). This analysis revealed that several integrins and ECMPs were differentially expressed in hNPCs than the other cell populations examined. To confirm the expression of specific integrins in hNPCs, we used flow cytometry to measure the cell surface expression of several α- and β-integrin subunits in proliferating hNPCs (Figure 1B). This analysis revealed that integrins α_4 (ITGA4), β_3 (ITGB3), β_4 (ITGB4), β_7 (ITGB7) were not expressed on the cell surface of

hNPCs. Integrin subunits α_1 (ITGA1), α_2 (ITGA2), α_3 (ITGA3), β_5 (ITGB5) were expressed at low levels while integrin subunits α_5 (ITGA5), α_6 (ITGA6), α_v (ITGAV), β_1 (ITGB1), β_2 (ITGB2) were highly expressed by proliferating hNPCs. Collectively, these integrin subunits can form the heterodimers $\alpha_1\beta_1$ (binds to collagen and laminin), $\alpha_2\beta_1$ (binds to collagen and laminin), $\alpha_3\beta_1$ (binds to collagen, laminin, and fibronectin), $\alpha_5\beta_1$ (binds to fibronectin), $\alpha_6\beta_1$ (binds to laminin), $\alpha_v\beta_1$ (binds to fibronectin), and $\alpha_v\beta_5$ (binds to fibronectin and vitronectin) (13).

Using this information about the specific ECMPs and integrins that were highly expressed in hNPCs, we designed a library of peptides with sequences that mimic these ECMPs or the active domains known to interact with these integrin heterodimers (28, 34–53) (Supplementary Table 1). To test if these peptides could support the growth and adhesion of hNPCs, cells were seeded into 96-well plates coated with 500 μM of each peptide. LN-coated 96-well plates were used as positive controls. Cell morphology (Figure 2A) and cell counts (Figure 2B) were analyzed after 72 hrs. Of the 18 peptides tested, only four peptides allowed for hNPCs to display a morphology and cell number similar to that of cells grown on laminin control surfaces—peptide 1 (laminin α1 derived, binds to integrins $\alpha_2\beta_1$ and $\alpha_6\beta_1$; (34, 35)), peptide 10 (laminin γ1 derived, binds to integrin $\alpha_6\beta_1$; (44, 46)), peptide 12 (vitronectin derived, binds to integrins $\alpha_5\beta_1$ and $\alpha_v\beta_5$; (47)), and peptide 13 (vitronectin derived, binds to integrins $\alpha_v\beta_5$: (28)).

3.2 Long-term expansion of hNPCs on defined peptide surfaces

We tested if the four ‘hit’ peptides that we identified to support the short-term growth of hNPCs could support hNPC attachment and growth over multiple passages. We cultured H9 hNPCs in 12-well plates coated with each ‘hit’ peptide. Cell detachment or differentiation, as indicated by acquisition of a neuronal morphology, was observed within the first three passages on peptides 1, 10, and 12 (Supplementary Figure 2). By comparison, hNPCs cultured on peptide 13 (herein referred to as vitronectin-derived peptide [VDP]) displayed a morphology and growth rate similar to those grown on LN control substrates (Supplementary Figure 2).

Next, we wanted to determine the minimum concentration of VDP that was required to promote hNPC adhesion at levels similar to that on LN-control substrates. To that end, H9 hNPCs were cultured in 12-well plates coated with 1, 10, 100, 200, and 500 μM VDP. VDP conjugated to a fluorescent dye (Figure 3A) was used to confirm that the amount of peptide absorbed onto the tissue culture surfaces decreased with the VDP concentration (Figure 3B and Figure 3C). This analysis revealed that 100 μM was the minimum concentration of VDP necessary to promote cell morphology (Figure 3C) and adhesion (Figure 3D) similar to that of hNPCs cultured on LN-control substrates. In addition, hNPCs did not adhere or displayed abnormal cell morphologies when cultured on uncoated or surfaces coated with other cationic peptides, such as poly-L-ornithine (PLO) (Supplementary Figure 3).

To investigate the broad utility of VDP as a hNPC culture substrate, we performed long-term culture analysis with four hNPC lines derived from three independent hESC lines (H9 (54), HSF4 (55), and HES3 (56)) and one hiPSC line (RiPSC (57)). HNPCs cultured on VDP-coated substrates maintained their characteristic morphology over 10 passages (> 50 days;

H9-hNPCs: Figure 4A; HSF4-, HES3-, and RiPSC-hNPCs: Supplementary Figure 4A). HNPCs cultured on VDP displayed a similar doubling time (H9-hNPCs: Figure 4B; RiPSC-hNPCs: Supplementary Figure 4) to cells cultured on control LN substrates. In addition, the hNPC growth rate on VDP remained constant over the course of 10 passages (H9-hNPCs: Figure 4C; RiPSC-hNPCs: Supplementary Figure 4C). Importantly, this growth analysis demonstrated that hNPCs cultured on VDP did not display an "adaptation phase" (i.e. slow growth during early passage on VDP) or growth senescence at higher passages. Cell counts taken at each passage revealed that 2 × 105 hNPCs could theoretically be expanded to 1×10^{11} over the course of 10 passages (H9-hNPCs: Figure 4C; RiPSC-hNPCs: Supplementary Figure 4C). Quantitative RT-PCR (qPCR) showed that there was no statistically significant difference in the expression of genes associated with a hNPC phenotoype (SOX1, SOX2, NESTIN) in hNPCs grown on VDP- and LN-coated surfaces throughout 10 passages (H9 hNPCs: Figure 4D; HSF4-hNPCs: Supplementary Figure 4D; RiPSC hNPCs: Supplementary Figure 4E). Similarly, immunofluorescence (H9 hNPCs: Figure 4E; RiPSC-hNPCs: Supplementary Figure 4F) and flow cytometry (H9-hNPCs: Figure 4F; HSF4-hNPCs: Supplementary Figure 4G; RiPSC-hNPCs: Supplementary Figure 4H) on passage 10 (p10) hNPCs demonstrated that a high percentage (>85%) of cells cultured on LN- and VDP-coated surfaces expressed the hNPC markers SOX1, SOX2, and NESTIN. In addition, this analysis revealed that there were no differences in the homogeneity of the hNPCs cultured on LN or VDP as both substrates supported cell populations that were >90% SOX1+SOX2+ (Figure 4F). Taken together, these results demonstrate that VDP is able to support the long-term expansion of several independently derived hNPC lines at similar levels to control LN substrates.

3.3 Characterization of hNPC attachment to VDP-coated surfaces

We hypothesized that long-term culture of hNPCs on VDP-coated surfaces would lead to a shift in their integrin expression profile from one that favors binding to LN (i.e. integrins α1, α2, α3, α6, β1) to one that favors binding to VDP (i.e. integrins αv, β3, β5) (28). To that end, we used qPCR and flow cytometry to measure the expression of these integrin subunits in RiPSC- (Figure 5A), H9- (Supplementary Figure 5A), and HES3-hNPCs (Supplementary Figure 5B) that had been cultured on LN and VDP substrates as well as surfaces coated with Matrigel™, an undefined, animal derived matrix that supports a variety of stem cell populations. Surprisingly, this analysis revealed no statistically significant differences in integrin expression between hNPCs cultured on VDP- and LN-coated surfaces. Because our initial analysis of endogenous ECMP expression revealed that several ECMPs, such as LN, are highly expressed by hNPCs compared to other cell populations tested (Figure 1A), we speculated that continued expression of laminin- and collagen-binding integrins that do not directly bind to VDP may facilitate interaction with endogenous ECMPs that are produced by hNPCs after their initial adhesion and subsequent growth. To that end, gene expression analysis reveal that hNPCs cultured on VDP for 10 passages expressed similarly high levels of LN (~100 fold greater than undifferentiated hPSCs) as hNPCs cultured on LN (Supplementary Figure 5C).

Previous studies have shown that in addition to integrins, cell adhesion molecules (CAMs) regulate pluripotent stem cell adhesion and differentiation (58). As such, we used qPCR and

flow cytometry to measure the expression of E-Cadherin, N-Cadherin, EpCAM, and NCAM in RiPSC- (Figure 5B), H9- (Supplementary Figure 5D), and HES3-hNPCs (Supplementary Figure 5E) that had been cultured on LN-, VDP-, and Matrigel™ coated substrates. As expected, flow cytometry analysis revealed that cell surface expression of the epithelial-related CAMs, E-Cadherin and EpCAM, was largely absent in hNPCs grown on all three substrates (Figure 5B). In addition, qPCR and flow cytometry analysis revealed that expression of the neural-related CAMs, N-Cadherin and NCAM, was similar in hNPCs grown on LN and VDP (Figure 5B; Supplementary Figure 5D and 5E).

Interestingly, flow cytometry analysis revealed, hNPCs cultured on Matrigel™-coated substrates expressed significantly higher levels of integrin subunits α1 and α2 (Figure 5A). Increased expression of these collagen binding subunits may facilitate hNPC interaction with the collagens that constitute a significant component of most Matrigel™ preparations (59). Along similar lines, flow cytometry analysis also revealed that cell surface expression of N-Cadherin and NCAM, was substantially reduced in hNPCs grown on Matrigel™ (Figure 5D) possibly due to the presence of numerous growth factors present in Matrigel™ known to influence hNPC fate (60).

Previous studies have demonstrated that VDP not only mediates cell binding through interactions with the vitronectin binding integrin α_v but also the glycosaminoglycan (GAG) side chain of cell surface proteoglycans (26). While addition of ethylenediamine tetra-acetic acid (EDTA), a general disruptor of integrin-mediated adhesion, reduced cell hNPC attachment to both LN and VDP substrates, the addition of an α_v blocking antibody only affected cell attachment to VDP substrates (Figure 6A and 6B). Additionally, our analysis revealed that hNPCs expressed several proteoglycans including decorin (*DCN*), fibromodulin (*FMOD*), lumican (*LUM*), and perlecan (*PLC*) (Supplementary Figure 6). To investigate whether the GAG side chain of these proteoglycans facilitated hNPC attachment to VDP, we treated hNPCs with soluble heparin (which competes with the GAG side chain of cell surface proteoglycans for adhesion to the substrate (61–63)). HNPC attachment to VDP was significantly reduced in the presence of soluble heparin (Figure 6A and 6B). Additionally, treatment with chondroitinase ABC (which catalyzes the enzymatic degradation of the GAG side chain of chondroitin sulfate proteoglycans) significantly reduced the level of hNPC adhesion to VDP-coated surfaces (Figure 6A and 6B). Together, these results suggest that VDP facilitates adhesion of hNPCs through the vitronectin binding integrin α_v as well as GAG side chain of cell surface proteoglycans.

3.4 Neuronal differentiation of hNPCs on VDP-coated surfaces

We next assessed if VDP surfaces could support the neuronal differentiation of hNPCs. HNPCs were grown on VDP and LN control surfaces until they reached confluence and neuronal differentiation medium was added. After 4 weeks of differentiation, cells cultured on VDP and LN substrates acquired a neuronal-like morphology. QPCR analysis revealed that when compared to the hNPC cultures expression of the pan-neuronal markers *β3T* and *MAP2* were significantly elevated in the neuronal cultures generated on both LN- and VDP-coated surfaces (H9-hNPCs: Figure 7A and 7B; HES3-hNPCs: Supplementary Figure 7A). Importantly, there was no statistically significant difference in expression of these markers in

neurons generated on LN substrates compared to neurons generated on VDP substrates. Along similar lines, immunofluorescence revealed that the percentage of cells that were positive for β3T, MAP2, neurofilament-68 (NF-L), and the neurotransmitter γ-aminobutyric acid (GABA) was similar in neuronal cultures generated on VDP and LN substrates (RiPSC hNPCS: Figure 7C–E; H9-hNPCs Supplementary Figure 7B). Finally, quantification of the raw number of β3T, MAP2, and NF-L positive cells revealed that VDP was an equally efficient differentiation substrate as LN (RiPSC-hNPCs: Figure 7F). Overall, these results demonstrate that VDP is a highly effective neuronal differentiation matrix for hNPCs.

4. DISCUSSION

The application of hNPCs for scientific and clinical purposes necessitates the engineering of completely defined and scalable substrates that support their long-term expansion and directed neuronal differentiation. In this study, we identified one peptide-based substrate, VDP, which was able to support the long-term growth of several independently derived hNPC lines over multiple passages in defined medium conditions. Compared to hNPCs cultured on ECMP-based LN substrates, hNPCs grown on VDP-coated surfaces displayed similar morphologies, growth rates, and high expression levels of hNPC multipotency markers. Furthermore, VDP surfaces supported the directed differentiation of hNPCs to neurons at similar levels to cells differentiated on LN substrates.

Laminin from tissue purified or recombinant sources is the most commonly used substrate for the growth and differentiation of hNPCs (19). The use of LN as a substrate for hNPC culture is largely based on previously developed methods for the propagation of primary fetal and adult neural stem cells (NSCs) (64), which express high levels of the LN binding integrins α6 and β1 (12, 65). However, we found that only two (peptide 1 and peptide 10) of the eleven peptides derived the cell binding domains of LN or known to interact with LN-binding integrin heterodimer $\alpha_6\beta_1$ supported the attachment of hNPCs, and none were able to support the long-term growth of hNPCs. Our integrin expression profiling revealed that in addition to these LN binding integrins, hNPCs also expressed high levels of integrins that bind other ECMPs such collagen (i.e. α_1, α_2, α_3), fibronectin (i.e. α_5) and vitronectin (i.e. α_v). Nonetheless, peptides derived from these integrin binding domains of collagen and fibronectin did not support the attachment of hNPCs. The two peptides (VDP and peptide 12) derived from vitronectin that we examined were able to support the attachment of hNPCs but only VDP was able to support the long-term culture of hNPCs. Previous studies have demonstrated that VDP not only mediates cell binding through interactions with integrin α_v but also the GAG side chains of cell surface proteoglycans (26). As such, our analysis revealed that interrupting these α_v- or GAG-mediated cell-substrate interactions significantly reduced hNPC adhesion to VDP. It should be noted that our analysis did not focus on identifying the particular class of proteoglycans or specific proteoglycan that mediated hNPC adhesion to VDP. Specifically, we showed that treatment with soluble heparin (which competes with heparin sulfate and chondroitin sulfate cell surface GAGs (62)) or chondroitinase ABC (which catalyzes the enzymatic degradation of the GAG side chain of chondroitin sulfate proteoglycans) significantly reduced the adhesion of hNPCs to VDP. However, future studies that examine the effects of knockdown of individual proteoglycans or enzymatic degradation (e.g. via keratinase and heparanase) of additional

classes of GAGs (61) are required to uncover the precise mechanisms by which these cell surface GAGs mediate hNPC adhesion to VDP. Nonetheless, we speculate the dual ability of VDP to bind to both integrin α_v as well as the GAG side chain of cell surface proteoglycans expressed by hNPCs allowed for VDP to uniquely support the long-term expansion of hNPCs.

The development of synthetic substrates for the culture of hPSCs and their derivatives has been explored by numerous groups (66, 67). Broadly, speaking these approaches can be classified into two groups—polymer- and peptide-based. Because polymer-based approaches have benefits such as cost and reproducibility, several groups, including our own, have developed polymer-based substrates for the growth and differentiation of hPSCs (66, 67). However, these polymer-based methods requires complex chemical approaches for conjugation to tissue culture surfaces and therefore are not widely accessible by researchers that do not have expertise with such methods. By comparison, peptide-based methods, such as VDP, have the tremendous benefits of off-the-shelf availability and ease of use as these peptides can be coated onto tissue culture surfaces in a manner similar to ECMPs such as LN. As such, peptide-based materials have been used for the expansion and differentiation of hPSCs (66, 68). In particular, a similar peptide sequence that served for the basis for VDP in this study has been used for the long-term culture of undifferentiated hPSCs (27). More recently, surfaces displaying this same peptide sequence supported the differentiation of hPSCs to early endoderm and mesoderm cell types (26). Interestingly, surfaces displaying similar peptide sequences to VDP only supported the ectodermal differentiation of hPSCs when those surfaces also displayed a cyclic-RGD containing peptide. Our analysis revealed several RGD binding integrins, such as integrin α_5, were expressed at significantly higher levels in early hPSC-derived ectoderm cells than in proliferating hNPCs possibly explaining the need for both peptide sequences for the differentiation of hPSCs to early ectoderm cell types. Another broadly used peptide-based material, Corning® Synthemax®, has been used for the long-term culture of hPSCs (24) as well as their differentiation into retinal pigmented epithelial cells (21), mesenchymal stem cells (22), oligodendrocyte progenitor cells (23), cardiomyocytes (24), and insulin producing cells (25). In this study, we tested the same peptide sequence (peptide 12) that serves as the basis for Corning® Synthemax®. Although this peptide was able to support the attachment and short-term expansion of hNPCs, it did not provide for the expansion of hNPCs over multiple passages. Moreover, Synthemax® plates purchased directly from Corning® were unable to support the long-term growth of hNPCs (data not shown).

Several groups have reported the use of peptide-based substrates for the short-term expansion of primary NSCs (69, 70). For example, Li et al. reported the use of laminin derived IKVAV peptide conjugated to gold-coated cover slips for the short-term growth and neuronal differentiation of immortalized human fetal NSCs (69). Along similar lines, Little et al. identified several RGD-based peptide surfaces that allowed for the adhesion, growth and differentiation of adult rat hippocampal NSCs (70). In this study, peptides containing IKVAV (peptide 4) and RGD (peptide 15) were unable to support the attachment and growth of hNPCs. Although NSCs derived from fetal (71–74) and adult (75–78) sources share some morphological, biochemical, and genetic similarities to hPSC-derived hNPCs, several studies have shown that the growth conditions and differentiation potential of these two cell

populations are quite different (64). These subtle biological differences could potentially explain why peptide surfaces that have been previously used for the culture of NSCs did not support the long-term culture of hNPCs. In addition, it should also be noted that all peptides used in this study were unmodified and coated onto tissue culture plates by simple absorption. Therefore, the inability of specific peptides to support hNPC adhesion and growth could be due incomplete coating onto tissue culture surfaces.

The development of robust, defined, and scalable substrates for hNPC culture and differentiation are necessary to realize their scientific and clinical potential. In this study, we demonstrate that VDP is a robust growth and differentiation matrix, as demonstrated by its ability to support the expansion and neuronal differentiation of hNPCs derived from three hESC (H9, HUES9, and HSF4) and one hiPSC (RiPSC) cell lines. In addition, similar to hNPCs grown on LN, cells expanded on VDP can be frozen and thawed without any detectable effects on their morphology, growth, and differentiation potential. Furthermore, similar to ECMPs, VDP can be easily coated onto TCPS plates and does not require immobilization by complex chemical modification or conjugation characteristic of other peptide-based culture systems (24, 69). Finally, in this study we show that VDP allows for the theoretical expansion of hNPCs to quantities ($>10^{10}$) necessary for drug screening or regenerative medicine purposes. In the future, VDP could potentially be used in microcarrier-based bioreactor systems (79) for the practical large-scale expansion and neuronal differentiation of hNPCs.

5. CONCLUSIONS

In this study, we developed a completely defined, scalable, and robust peptide-based substrate that allows for the long-term growth and directed neuronal differentiation of hNPCs. Compared to cells grown on standard LN-based substrates, hNPCs grown on VDP maintained their characteristic morphology, expressed high levels of hNPC multipotency markers, and retained their neuronal differentiation potential. In the future, the use of VDP as a defined culture substrate will significantly advance the clinical application of hNPCs and their derivatives as it will enable the large-scale expansion and neuronal differentiation of hNPCs in quantities necessary for disease modeling, drug screening, and regenerative medicine applications.

Supplementary Material

Refer to Web version on PubMed Central for supplementary material.

Acknowledgments

The research was supported by funding from the Arizona Alzheimer's Consortium, an ASU/Mayo Seed Grant, and the NIH (5R21EB020767).

References

1. Lindvall O, Kokaia Z. Stem cells for the treatment of neurological disorders. Nature. 2006; 441:1094–1096. [PubMed: 16810245]

2. Lindvall O, Kokaia Z. Stem cells in human neurodegenerative disorders--time for clinical translation? J Clin Invest. 2010; 120:29–40. [PubMed: 20051634]
3. Casarosa S, Bozzi Y, Conti L. Neural stem cells: ready for therapeutic applications? Mol Cell Ther. 2014; 2:31. [PubMed: 26056597]
4. Zhang SC, Li XJ, Johnson MA, Pankratz MT. Human embryonic stem cells for brain repair? Philos Trans R Soc Lond B Biol Sci. 2008; 363:87–99. [PubMed: 17322002]
5. Koch P, Kokaia Z, Lindvall O, Brustle O. Emerging concepts in neural stem cell research: autologous repair and cell-based disease modelling. Lancet Neurol. 2009; 8:819–829. [PubMed: 19679274]
6. Ruggieri M, Riboldi G, Brajkovic S, Bucchia M, Bresolin N, Comi GP, Corti S. Induced neural stem cells: methods of reprogramming and potential therapeutic applications. Prog Neurobiol. 2013; 114:15–24. [PubMed: 24246715]
7. Bretzner F, Gilbert F, Baylis F, Brownstone RM. Target populations for first-in-human embryonic stem cell research in spinal cord injury. Cell Stem Cell. 2011; 8:468–475. [PubMed: 21549321]
8. Schwartz SD, Hubschman JP, Heilwell G, Franco-Cardenas V, Pan CK, Ostrick RM, Mickunas E, Gay R, Klimanskaya I, Lanza R. Embryonic stem cell trials for macular degeneration: a preliminary report. Lancet. 2012; 379:713–720. [PubMed: 22281388]
9. Sterneckert JL, Reinhardt P, Scholer HR. Investigating human disease using stem cell models. Nat Rev Genet. 2014; 15:625–639. [PubMed: 25069490]
10. Marchetto MC, Winner B, Gage FH. Pluripotent stem cells in neurodegenerative and neurodevelopmental diseases. Hum Mol Genet. 2010; 19:R71–76. [PubMed: 20418487]
11. Warren HS, Tompkins RG, Moldawer LL, Seok J, Xu W, Mindrinos MN, Maier RV, Xiao W, Davis RW. Mice are not men. Proc Natl Acad Sci U S A. 2014; 112:E345. [PubMed: 25540422]
12. Hall PE, Lathia JD, Miller NG, Caldwell MA, ffrench-Constant C. Integrins are markers of human neural stem cells. Stem Cells. 2006; 24:2078–2084. [PubMed: 16690778]
13. Humphries JD, Byron A, Humphries MJ. Integrin ligands at a glance. J Cell Sci. 2006; 119:3901–3903. [PubMed: 16988024]
14. Brizzi MF, Tarone G, Defilippi P. Extracellular matrix, integrins, and growth factors as tailors of the stem cell niche. Curr Opin Cell Biol. 2012; 24:645–651. [PubMed: 22898530]
15. Laperle A, Masters KS, Palecek SP. Influence of substrate composition on human embryonic stem cell differentiation and extracellular matrix production in embryoid bodies. Biotechnol Prog. 2014; 31:212–219. [PubMed: 25311359]
16. Ma W, Tavakoli T, Derby E, Serebryakova Y, Rao MS, Mattson MP. Cell-extracellular matrix interactions regulate neural differentiation of human embryonic stem cells. BMC Dev Biol. 2008; 8:90. [PubMed: 18808690]
17. Brafman DA, Phung C, Kumar N, Willert K. Regulation of endodermal differentiation of human embryonic stem cells through integrin-ECM interactions. Cell Death Differ. 2013; 20:369–381. [PubMed: 23154389]
18. Brafman DA, Shah KD, Fellner T, Chien S, Willert K. Defining long-term maintenance conditions of human embryonic stem cells with arrayed cellular microenvironment technology. Stem Cells Dev. 2009; 18:1141–1154. [PubMed: 19327010]
19. Koch P, Opitz T, Steinbeck JA, Ladewig J, Brustle O. A rosette-type, self-renewing human ES cell-derived neural stem cell with potential for in vitro instruction and synaptic integration. Proc Natl Acad Sci U S A. 2009; 106:3225–3230. [PubMed: 19218428]
20. Chambers SM, Fasano CA, Papapetrou EP, Tomishima M, Sadelain M, Studer L. Highly efficient neural conversion of human ES and iPS cells by dual inhibition of SMAD signaling. Nat Biotechnol. 2009; 27:275–280. [PubMed: 19252484]
21. Pennington BO, Clegg DO, Melkoumian ZK, Hikita ST. Defined culture of human embryonic stem cells and xeno-free derivation of retinal pigmented epithelial cells on a novel, synthetic substrate. Stem Cells Transl Med. 2015; 4:165–177. [PubMed: 25593208]
22. Dolley-Sonneville PJ, Romeo LE, Melkoumian ZK. Synthetic surface for expansion of human mesenchymal stem cells in xeno-free, chemically defined culture conditions. PLoS One. 2013; 8:e70263. [PubMed: 23940553]

23. Li Y, Gautam A, Yang J, Qiu L, Melkoumian Z, Weber J, Telukuntla L, Srivastava R, Whiteley EM, Brandenberger R. Differentiation of oligodendrocyte progenitor cells from human embryonic stem cells on vitronectin-derived synthetic peptide acrylate surface. Stem Cells Dev. 2012; 22:1497–1505.
24. Melkoumian Z, Weber JL, Weber DM, Fadeev AG, Zhou Y, Dolley-Sonneville P, Yang J, Qiu L, Priest CA, Shogbon C, Martin AW, Nelson J, West P, Beltzer JP, Pal S, Brandenberger R. Synthetic peptide-acrylate surfaces for long-term self-renewal and cardiomyocyte differentiation of human embryonic stem cells. Nat Biotechnol. 2010; 28:606–610. [PubMed: 20512120]
25. Lin PY, Hung SH, Yang YC, Liao LC, Hsieh YC, Yen HJ, Lu HE, Lee MS, Chu IM, Hwang SM. A synthetic peptide-acrylate surface for production of insulin-producing cells from human embryonic stem cells. Stem Cells Dev. 2013; 23:372–379. [PubMed: 24083371]
26. Wrighton PJ, Klim JR, Hernandez BA, Koonce CH, Kamp TJ, Kiessling LL. Signals from the surface modulate differentiation of human pluripotent stem cells through glycosaminoglycans and integrins. Proc Natl Acad Sci U S A. 2014; 111:18126–18131. [PubMed: 25422477]
27. Klim JR, Li L, Wrighton PJ, Piekarczyk MS, Kiessling LL. A defined glycosaminoglycan-binding substratum for human pluripotent stem cells. Nat Methods. 2010; 7:989–994. [PubMed: 21076418]
28. Vogel BE, Lee SJ, Hildebrand A, Craig W, Pierschbacher MD, Wong-Staal F, Ruoslahti E. A novel integrin specificity exemplified by binding of the alpha v beta 5 integrin to the basic domain of the HIV Tat protein and vitronectin. J Cell Biol. 1993; 121:461–468. [PubMed: 7682219]
29. Kumar N, Richter J, Cutts J, Bush KT, Trujillo C, Nigam SK, Gaasterland T, Brafman D, Willert K. Generation of an expandable intermediate mesoderm restricted progenitor cell line from human pluripotent stem cells. Elife. 2015; 4
30. Moya N, Cutts J, Gaasterland T, Willert K, Brafman DA. Endogenous WNT Signaling Regulates hPSC-Derived Neural Progenitor Cell Heterogeneity and Specifies Their Regional Identity. Stem Cell Reports. 2014
31. Yuan SH, Martin J, Elia J, Flippin J, Paramban RI, Hefferan MP, Vidal JG, Mu Y, Killian RL, Israel MA, Emre N, Marsala S, Marsala M, Gage FH, Goldstein LS, Carson CT. Cell-surface marker signatures for the isolation of neural stem cells, glia and neurons derived from human pluripotent stem cells. PLoS One. 2011; 6:e17540. [PubMed: 21407814]
32. VanGuilder HD, Vrana KE, Freeman WM. Twenty-five years of quantitative PCR for gene expression analysis. Biotechniques. 2008; 44:619–626. [PubMed: 18474036]
33. Kim SH, Turnbull J, Guimond S. Extracellular matrix and cell signalling: the dynamic cooperation of integrin, proteoglycan and growth factor receptor. J Endocrinol. 2011; 209:139–151. [PubMed: 21307119]
34. Nomizu M, Kim WH, Yamamura K, Utani A, Song SY, Otaka A, Roller PP, Kleinman HK, Yamada Y. Identification of cell binding sites in the laminin alpha 1 chain carboxyl-terminal globular domain by systematic screening of synthetic peptides. J Biol Chem. 1995; 270:20583–20590. [PubMed: 7657636]
35. Nakahara H, Nomizu M, Akiyama SK, Yamada Y, Yeh Y, Chen WT. A mechanism for regulation of melanoma invasion. Ligation of alpha6beta1 integrin by laminin G peptides. J Biol Chem. 1996; 271:27221–27224. [PubMed: 8910291]
36. Tashiro K, Monji A, Yoshida I, Hayashi Y, Matsuda K, Tashiro N, Mitsuyama Y. An IKLLI-containing peptide derived from the laminin alpha1 chain mediating heparin-binding, cell adhesion, neurite outgrowth and proliferation, represents a binding site for integrin alpha3beta1 and heparan sulphate proteoglycan. Biochem J. 1999; 340(Pt 1):119–126. [PubMed: 10229666]
37. Siqueira AS, Gama-de-Souza LN, Arnaud MV, Pinheiro JJ, Jaeger RG. Laminin-derived peptide AG73 regulates migration, invasion, and protease activity of human oral squamous cell carcinoma cells through syndecan-1 and beta1 integrin. Tumour Biol. 2010; 31:46–58. [PubMed: 20237901]
38. Nomizu M, Kuratomi Y, Malinda KM, Song SY, Miyoshi K, Otaka A, Powell SK, Hoffman MP, Kleinman HK, Yamada Y. Cell binding sequences in mouse laminin alpha1 chain. J Biol Chem. 1998; 273:32491–32499. [PubMed: 9829982]
39. Freitas VM, Vilas-Boas VF, Pimenta DC, Loureiro V, Juliano MA, Carvalho MR, Pinheiro JJ, Camargo AC, Moriscot AS, Hoffman MP, Jaeger RG. SIKVAV, a laminin alpha1-derived peptide,

interacts with integrins and increases protease activity of a human salivary gland adenoid cystic carcinoma cell line through the ERK 1/2 signaling pathway. Am J Pathol. 2007; 171:124–138. [PubMed: 17591960]

40. Maeda T, Titani K, Sekiguchi K. Cell-adhesive activity and receptor-binding specificity of the laminin-derived YIGSR sequence grafted onto Staphylococcal protein A. J Biochem. 1994; 115:182–189. [PubMed: 8206865]
41. Charonis AS, Skubitz AP, Koliakos GG, Reger LA, Dege J, Vogel AM, Wohlhueter R, Furcht LT. A novel synthetic peptide from the B1 chain of laminin with heparin-binding and cell adhesion-promoting activities. J Cell Biol. 1988; 107:1253–1260. [PubMed: 3417782]
42. Skubitz AP, McCarthy JB, Zhao Q, Yi XY, Furcht LT. Definition of a sequence, RYVVLPR, within laminin peptide F-9 that mediates metastatic fibrosarcoma cell adhesion and spreading. Cancer Res. 1990; 50:7612–7622. [PubMed: 2253210]
43. Liesi P, Narvanen A, Soos J, Sariola H, Snounou G. Identification of a neurite outgrowth-promoting domain of laminin using synthetic peptides. FEBS Lett. 1989; 244:141–148. [PubMed: 2924902]
44. Nomizu M, Kuratomi Y, Song SY, Ponce ML, Hoffman MP, Powell SK, Miyoshi K, Otaka A, Kleinman HK, Yamada Y. Identification of cell binding sequences in mouse laminin gamma1 chain by systematic peptide screening. J Biol Chem. 1997; 272:32198–32205. [PubMed: 9405421]
45. Ponce ML, Nomizu M, Kleinman HK. An angiogenic laminin site and its antagonist bind through the alpha(v)beta3 and alpha5beta1 integrins. FASEB J. 2001; 15:1389–1397. [PubMed: 11387236]
46. Murayama O, Nishida H, Sekiguchi K. Novel peptide ligands for integrin alpha 6 beta 1 selected from a phage display library. J Biochem. 1996; 120:445–451. [PubMed: 8889832]
47. Suzuki S, Oldberg A, Hayman EG, Pierschbacher MD, Ruoslahti E. Complete amino acid sequence of human vitronectin deduced from cDNA. Similarity of cell attachment sites in vitronectin and fibronectin. EMBO J. 1985; 4:2519–2524. [PubMed: 2414098]
48. Woods A, McCarthy JB, Furcht LT, Couchman JR. A synthetic peptide from the COOH-terminal heparin-binding domain of fibronectin promotes focal adhesion formation. Mol Biol Cell. 1993; 4:605–613. [PubMed: 8374170]
49. Sharma A, Askari JA, Humphries MJ, Jones EY, Stuart DI. Crystal structure of a heparin- and integrin-binding segment of human fibronectin. EMBO J. 1999; 18:1468–1479. [PubMed: 10075919]
50. Haverstick DM, Cowan JF, Yamada KM, Santoro SA. Inhibition of platelet adhesion to fibronectin, fibrinogen, and von Willebrand factor substrates by a synthetic tetrapeptide derived from the cell-binding domain of fibronectin. Blood. 1985; 66:946–952. [PubMed: 3876125]
51. Wang X, Lessman CA, Taylor DB, Gartner TK. Fibronectin peptide DRVPHSRNSIT and fibronectin receptor peptide DLYYLMDL arrest gastrulation of Rana pipiens. Experientia. 1995; 51:1097–1102. [PubMed: 7498451]
52. Danen EH, Aota S, van Kraats AA, Yamada KM, Ruiter DJ, van Muijen GN. Requirement for the synergy site for cell adhesion to fibronectin depends on the activation state of integrin alpha 5 beta 1. J Biol Chem. 1995; 270:21612–21618. [PubMed: 7545166]
53. Staatz WD, Fok KF, Zutter MM, Adams SP, Rodriguez BA, Santoro SA. Identification of a tetrapeptide recognition sequence for the alpha 2 beta 1 integrin in collagen. J Biol Chem. 1991; 266:7363–7367. [PubMed: 2019571]
54. Thomson JA, Itskovitz-Eldor J, Shapiro SS, Waknitz MA, Swiergiel JJ, Marshall VS, Jones JM. Embryonic stem cell lines derived from human blastocysts. Science. 1998; 282:1145–1147. [PubMed: 9804556]
55. Chavez SL, Meneses JJ, Nguyen HN, Kim SK, Pera RA. Characterization of six new human embryonic stem cell lines (HSF7, -8, -9, -10, -12, and -13) derived under minimal-animal component conditions. Stem Cells Dev. 2008; 17:535–546. [PubMed: 18513167]
56. Sidhu KS, Tuch BE. Derivation of three clones from human embryonic stem cell lines by FACS sorting and their characterization. Stem Cells Dev. 2006; 15:61–69. [PubMed: 16522163]
57. Warren L, Manos PD, Ahfeldt T, Loh YH, Li H, Lau F, Ebina W, Mandal PK, Smith ZD, Meissner A, Daley GQ, Brack AS, Collins JJ, Cowan C, Schlaeger TM, Rossi DJ. Highly efficient

reprogramming to pluripotency and directed differentiation of human cells with synthetic modified mRNA. Cell Stem Cell. 2010; 7:618–630. [PubMed: 20888316]

58. Li L, Bennett SA, Wang L. Role of E-cadherin and other cell adhesion molecules in survival and differentiation of human pluripotent stem cells. Cell Adh Migr. 2012; 6:59–70. [PubMed: 22647941]
59. Hughes CS, Radan L, Betts D, Postovit LM, Lajoie GA. Proteomic analysis of extracellular matrices used in stem cell culture. Proteomics. 2011; 11:3983–3991. [PubMed: 21834137]
60. Vukicevic S, Kleinman HK, Luyten FP, Roberts AB, Roche NS, Reddi AH. Identification of multiple active growth factors in basement membrane Matrigel suggests caution in interpretation of cellular activity related to extracellular matrix components. Exp Cell Res. 1992; 202:1–8. [PubMed: 1511725]
61. Iozzo RV, Schaefer L. Proteoglycan form and function: A comprehensive nomenclature of proteoglycans. Matrix Biol. 2015; 42:11–55. [PubMed: 25701227]
62. Hoffman MP, Engbring JA, Nielsen PK, Vargas J, Steinberg Z, Karmand AJ, Nomizu M, Yamada Y, Kleinman HK. Cell type-specific differences in glycosaminoglycans modulate the biological activity of a heparin-binding peptide (RKRLQVQLSIRT) from the G domain of the laminin alpha1 chain. J Biol Chem. 2001; 276:22077–22085. [PubMed: 11304538]
63. San Antonio JD, Lander AD, Wright TC, Karnovsky MJ. Heparin inhibits the attachment and growth of Balb/c-3T3 fibroblasts on collagen substrata. J Cell Physiol. 1992; 150:8–16. [PubMed: 1730788]
64. Conti L, Cattaneo E. Neural stem cell systems: physiological players or in vitro entities? Nat Rev Neurosci. 2010; 11:176–187. [PubMed: 20107441]
65. Pan L, North HA, Sahni V, Jeong SJ, McGuire TL, Berns EJ, Stupp SI, Kessler JA. beta1-Integrin and integrin linked kinase regulate astrocytic differentiation of neural stem cells. PLoS One. 2014; 9:e104335. [PubMed: 25098415]
66. Celiz AD, Smith JG, Langer R, Anderson DG, Winkler DA, Barrett DA, Davies MC, Young LE, Denning C, Alexander MR. Materials for stem cell factories of the future. Nat Mater. 2014; 13:570–579. [PubMed: 24845996]
67. Jordahl JH, Villa-Diaz LG, Kreshbach PH, Lahann J. Engineered Human Stem Cell Microenvironments. Curr Stem Cell Reports. 2016; 2:73–84.
68. Higuchi A, Kao SH, Ling QD, Chen YM, Li HF, Alarfaj AA, Munusamy MA, Murugan K, Chang SC, Lee HC, Hsu ST, Kumar SS, Umezawa A. Long-term xeno-free culture of human pluripotent stem cells on hydrogels with optimal elasticity. Sci Re. 2015; 5:18136.
69. Li X, Liu X, Josey B, Chou CJ, Tan Y, Zhang N, Wen X. Short laminin peptide for improved neural stem cell growth. Stem Cells Transl Med. 2014; 3:662–670. [PubMed: 24692587]
70. Little LE, Dane KY, Daugherty PS, Healy KE, Schaffer DV. Exploiting bacterial peptide display technology to engineer biomaterials for neural stem cell culture. Biomaterials. 2011; 32:1484–1494. [PubMed: 21129772]
71. Ciccolini F. Identification of two distinct types of multipotent neural precursors that appear sequentially during CNS development. Mol Cell Neurosci. 2001; 17:895–907. [PubMed: 11358486]
72. Ciccolini F, Svendsen CN. Fibroblast growth factor 2 (FGF-2) promotes acquisition of epidermal growth factor (EGF) responsiveness in mouse striatal precursor cells: identification of neural precursors responding to both EGF and FGF-2. J Neurosci. 1998; 18:7869–7880. [PubMed: 9742155]
73. Louis SA, Reynolds BA. Generation and differentiation of neurospheres from murine embryonic day 14 central nervous system tissue. Methods Mol Biol. 2005; 290:265–280. [PubMed: 15361668]
74. Tropepe V, Sibilia M, Ciruna BG, Rossant J, Wagner EF, van der Kooy D. Distinct neural stem cells proliferate in response to EGF and FGF in the developing mouse telencephalon. Dev Biol. 1999; 208:166–188. [PubMed: 10075850]
75. Reynolds BA, Weiss S. Generation of neurons and astrocytes from isolated cells of the adult mammalian central nervous system. Science. 1992; 255:1707–1710. [PubMed: 1553558]

76. Doetsch F, Petreanu L, Caille I, Garcia-Verdugo JM, Alvarez-Buylla A. EGF converts transit-amplifying neurogenic precursors in the adult brain into multipotent stem cells. Neuron. 2002; 36:1021–1034. [PubMed: 12495619]

77. Palmer TD, Takahashi J, Gage FH. The adult rat hippocampus contains primordial neural stem cells. Mol Cell Neurosci. 1997; 8:389–404. [PubMed: 9143557]

78. Palmer TD, Schwartz PH, Taupin P, Kaspar B, Stein SA, Gage FH. Cell culture. Progenitor cells from human brain after death. Nature. 2001; 411:42–43. [PubMed: 11333968]

79. Chen AK, Reuveny S, Oh SK. Application of human mesenchymal and pluripotent stem cell microcarrier cultures in cellular therapy: Achievements and future direction. Biotechnol Adv. 2013; 31:1032–1046. [PubMed: 23531528]

STATEMENT OF SIGNIFICANCE

In this study, we used a rational design process to develop a completely defined synthetic peptide-based substrate that allows for the robust long-term growth and neuronal differentiation of human neural progenitor cells (hNPCs) derived from multiple independent human pluripotent stem cells (hPSCs) lines. In addition, VDP can be simply coated onto tissue culture surfaces, thereby facilitating the ease of use by a wide variety of research groups. Finally, this work is significant as it will facilitate the large-scale expansion and neuronal differentiation of hNPCs in quantities necessary for clinical applications in disease modeling, drug screening, and regenerative medicine.

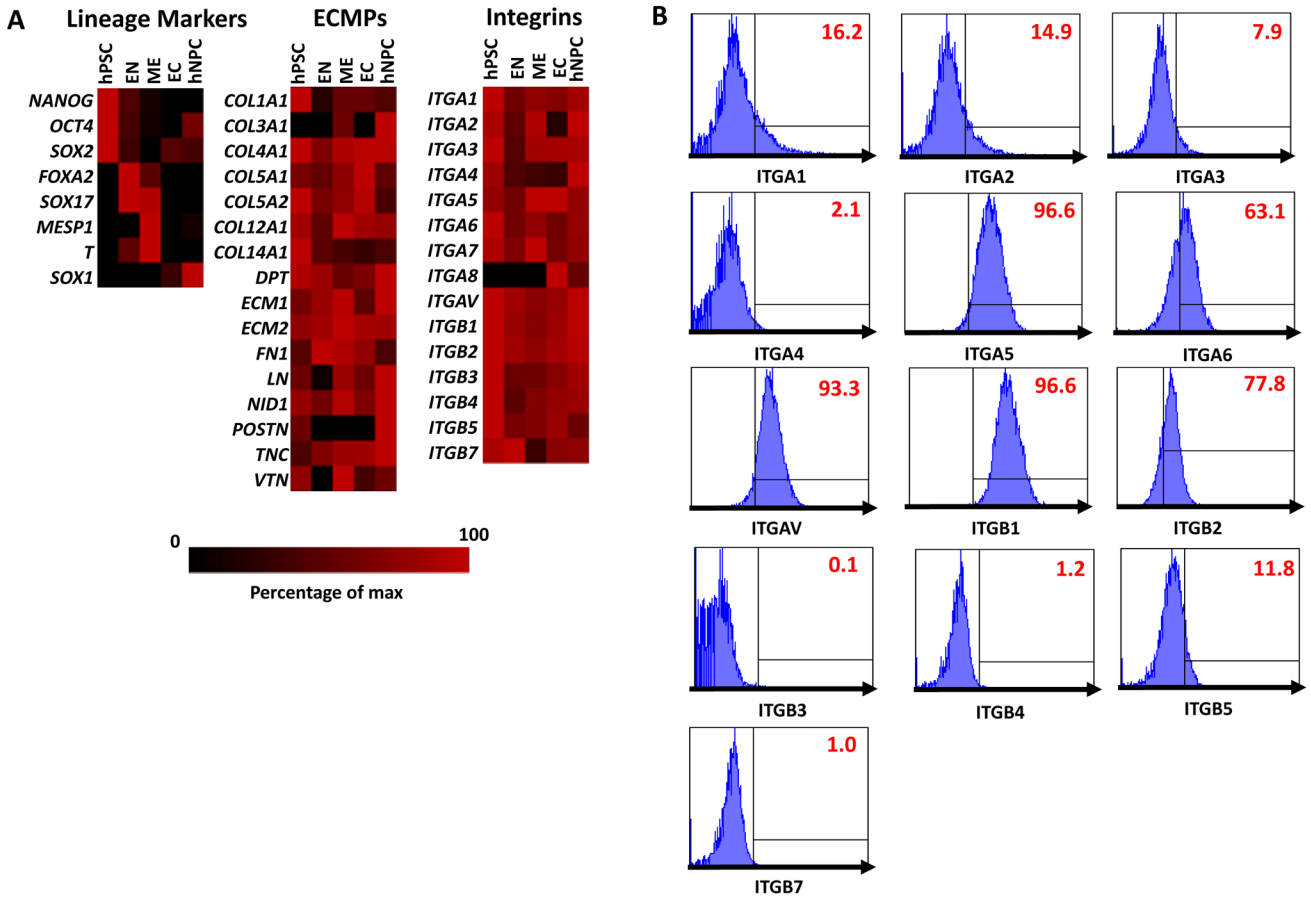

Figure 1. Analysis of extracellular matrix protein (ECMP) and integrin expression in hPSCs, hNPCs, and hPSC-derived endoderm (EN), mesoderm (ME), ectoderm (EC)

(A) Quantitative PCR analysis for expression of ECMPs and integrins in hPSCs, hNPCs, and transient EC, EN, ME cell populations differentiated from hPSCs. The data is displayed in a heat map where black corresponds to minimum expression levels and red corresponds to maximum levels. For each gene analyzed, the expression levels were normalized to the sample with the highest expression level. (B) Expression of integrins α1–6,β and β1–5,7 was measured in multipotent hNPCs was analyzed by flow cytometry. Gates were determined using isotype controls. Isotype controls used are listed in Supplementary Table 3.

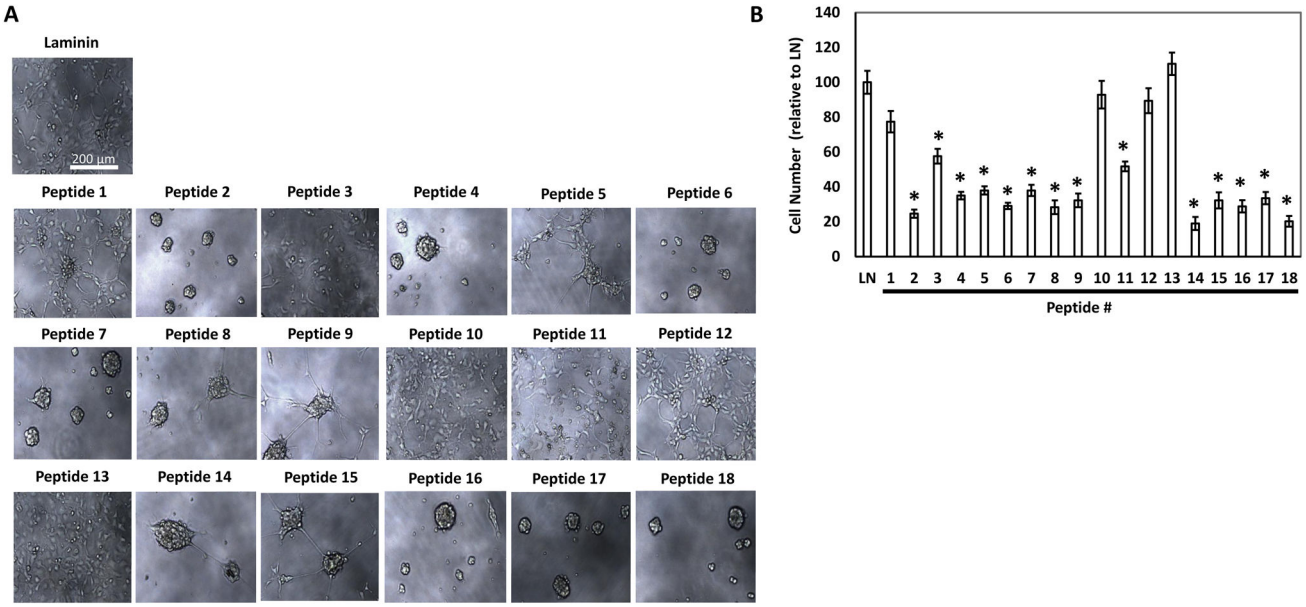

Figure 2. Identification of peptide-based surfaces for hNPC adhesion and growth

(A) Representative phase contrast images of H9-hNPCs cultured on laminin (LN)- or peptide-coated tissue culture plates for 72 hrs. All peptides were tested at a concentration of 0.5 µM. (B) Cell count of H9-hNPCs cultured on the LN or peptide-coated tissue culture plates for 72 hrs. Cell counts were normalized to those on LN surfaces. Data is presented as the mean ± standard deviation (S.D.). Cell counts on peptides were compared to cell counts on LN controls using Student's t-test with Bonferroni correction (*$p < 0.05$). The sequences of the peptides tested are listed in Supplementary Table 1.

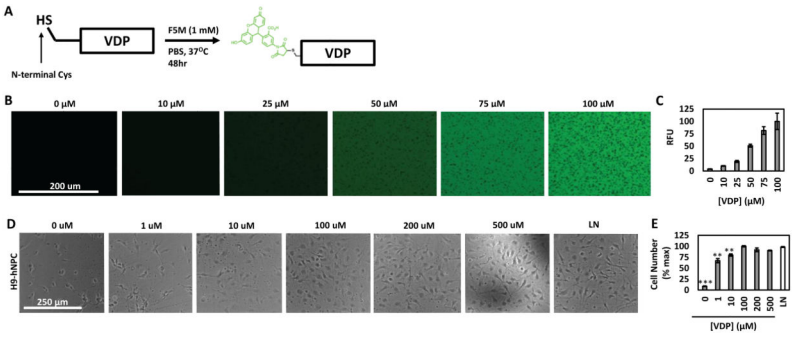

Figure 3. Effect of VDP concentration on growth and adhesion of hNPCs

(A) Schematic of protocol to covalently modify VDP with fluorescein-5-maleimide (F5M). (B) Representative fluorescent images of surfaces coated with VDP (at indicated concentrations) covalently modified with F5M (scale bar = 200 μm). (C) Quantification of F5M-labeled VDP adsorption onto tissue culture surfaces. Data is presented as the mean ± S.E.M. (D) Representative phase contrast images of H9-hNPCs grown on surfaces coated with various concentrations of VDP (scale = 250 μm). (E) Cell counts were performed after 72 hours of culture on the VDP-coated surfaces. Data is presented as the mean ± S.E.M. All comparisons were made to cell counts obtained on LN cultures using Student's t-test (** $p < 0.01$, ***$p<0.001$).

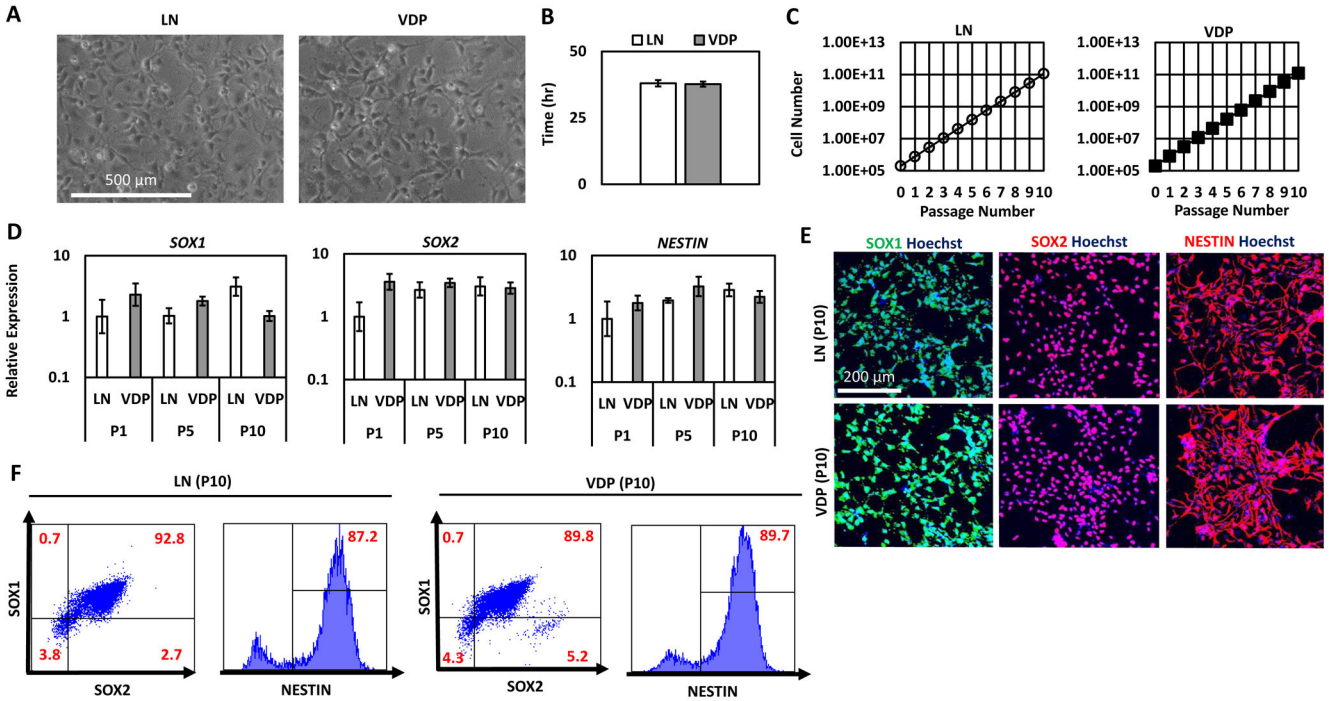

Figure 4. Long-term expansion of hNPCs on VDP-coated surfaces

(A) Representative phase contrast images of H9-hNPCs cultured on LN and VDP surfaces for 10 passages (scale bar = 500 µm). (B) Doubling time of H9-hNPCs cultured on LN and VDP. Data is presented as the mean ± S.D of the doubling time over the course of 10 passages. There was no statistical difference in the doubling time of hNPCs grown on LN and VDP (Student's t-test, p>0.05) (C) H9-hNPCs were cultured on LN and VDP and cell growth was analyzed by cell count at each passage (mean ± S.E.M). (D) Quantitative PCR analysis for expression of hNPC multipotency markers *SOX1*, *SOX2*, and *NESTIN* in H9-hNPCs cultured on LN and VDP for 1, 5, and 10 passages (mean ± S.E.M). Two-way analysis of variance (ANOVA) revealed that there was no statistical difference (p>0.05) in expression of these genes over the course of 10 passages in hNPCs cultured on LN- or VDP-coated surfaces. (E) SOX1, SOX2, and NESTIN immunofluorescence of H9-hNPCs cultured on LN and VDP for 10 passages (scale bar = 200 µm). (F) Flow cytometry analysis for SOX1, SOX2, and NESTIN expression in H9 hNPCs cultured on LN and VDP for 10 passages. Gates were determined using isotype controls. Isotype controls used are listed in Supplementary Table 3.

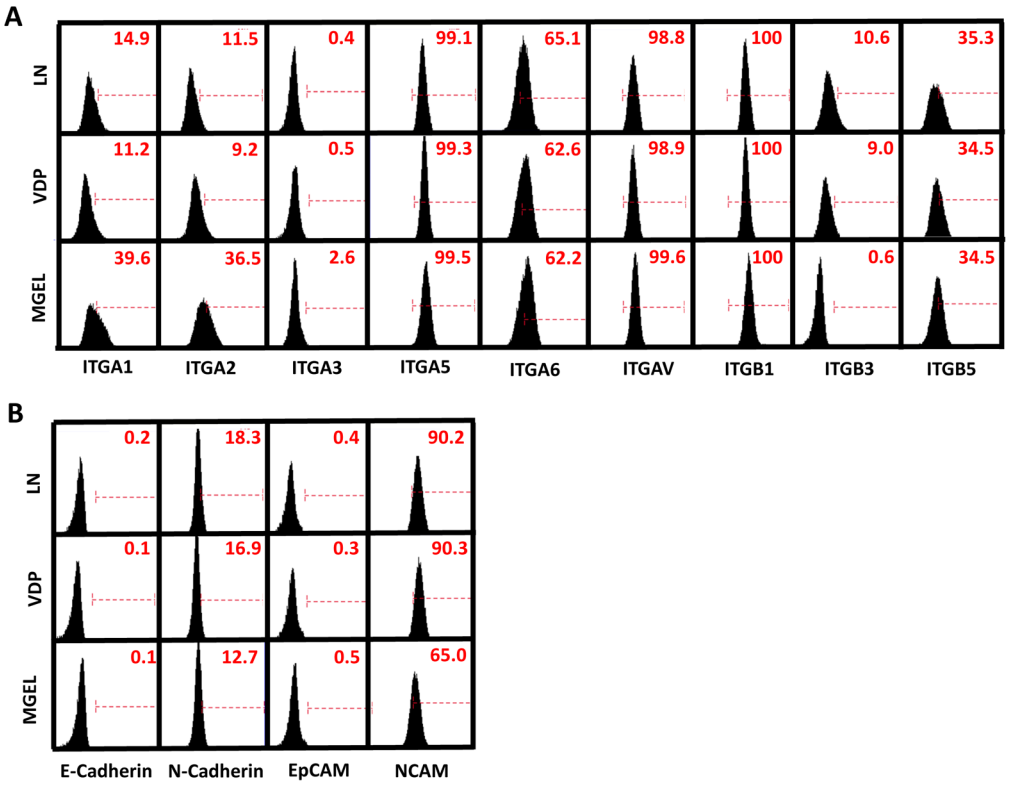

Figure 5. Analysis of integrin and cell adhesion molecule (CAM) expression of hNPCs cultured on LN-, VDP-, and Matrigel™-coated surfaces

Flow cytometry of cell surface expression of various (A) integrin subunits and (B) CAMs of RiPSC-hNPCs cultured on LN, VDP, or Matrigel™. Gates were determined using isotype controls. Isotype controls used are listed in Supplementary Table 3.

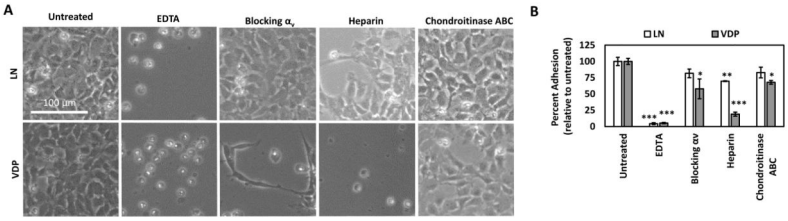

Figure 6. HNPC adhesion to VDP is mediated through integrin- and proteoglycan-dependent interactions

(A) Phase contrast images of RiPSC-hNPCs treated with EDTA, integrin α_V blocking antibody, heparin, and chondroitinase ABC prior to culture on LN- and VDP surfaces. (B) Cell counts were performed after 48 hours of culture. Data is presented as the mean ± S.E.M relative to untreated samples. All comparisons were made to untreated samples using Student's t-test (*p< 0.05, **p < 0.01, ***p<0.001).

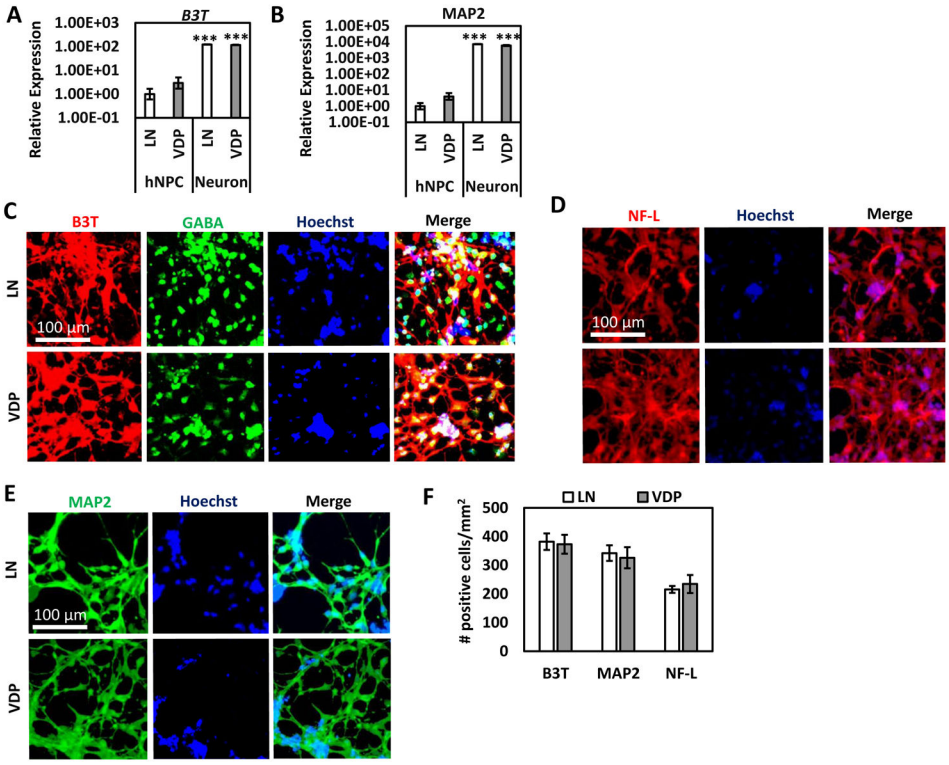

Figure 7. Neuronal differentiation of hNPCs of VDP-coated surfaces

Quantitative PCR analysis for expression of neuronal markers (A) *B3T* and (B) *MAP2* of neurons differentiated from H9-hNPCs on VDP and LN substrates (mean ± S.E.M). Expression of these genes was statistically significantly higher in the neuronal cultures compared to hNPCs for cells cultured on both substrates (Student's t-test, ***$p<0.001$). There was no statistically significant (Student's t-test, $p>0.05$) difference between expression of these genes in neuronal cultures generated on LN- and VDP-coated surfaces. Immunofluorescence for (C) B3T and GABA (D) NF-L, and (E) MAP2 on neurons differentiated from RiPSC-hNPCs on LN and VDP substrates (scale bar = 100 μM). (F) Cell counts of the number of B3T, MAP2, and NF-L positive cells in neuronal cultures generated from RiPSC-hNPCs on LN and VDP substrates (mean ± S.E.M). There was no statistically significant (Student's t-test, $p>0.05$) difference in the number of B3T, MAP2, and NF-L positive neurons generated on LN- and VDP-coated substrates.